DALTON
FULL PAPER

Synthesis and dynamic NMR studies of fluxionality in rhenium(I), platinum(II) and platinum(IV) complexes of 'back-to-back' 2,2′:6′,2″-terpyridine ligands

Andrew Gelling, Matthew D. Olsen, Keith G. Orrell,* Anthony G. Osborne and Vladimir Šik

Department of Chemistry, The University, Exeter, UK EX4 4QD.
E-mail: K.G.Orrell@exeter.ac.uk

Received 8th July 1998, Accepted 20th August 1998

Syntheses are given for the following transition metal complexes, $[\{ReBr(CO)_3\}_2L]$ (L = L^1, L^2 or L^3), $[(PtClMe_3)_2L^1]$, $[(PtIMe_3)_2L]$ (L = L^2 or L^3), $[ReBr(CO)_3L^1]$, $[Pt(C_6F_5)_2L^3]$, $[Pt(C_6F_4CF_3)_2L]$ (L = L^1 or L^2), $[\{Pt(C_6F_4CF_3)_2\}_2L]$ (L = L^1 or L^2) and $[ReBr(CO)_3PtIMe_3L^1]$ where the ligands, L, are the 'back-to-back' terpyridine ligands, 6′,6″-bis(2-pyridyl)-2,2′:4′,4″:2″,2‴-quaterpyridine (L^1), 1,4-bis(2,2′:6′,2″-terpyridin-4′-yl)benzene (L^2) and 6′,6″-bis{2-(4-methylpyridyl)}-2,2′:4′,4″:2″,2‴-quaterpyridine (L^3). All the complexes undergo 1,4-metallotropic shifts in solution at above-ambient temperatures and restricted rotations of the pendant pyridyl rings at below-ambient temperatures. Activation energies for these processes have been computed from variable temperature one-dimensional bandshape analysis and 2D-exchange spectroscopy (2D-EXSY) NMR experiments. The metallotropic shift energies are very metal-dependent being in the order $Pt^{IV} < Re^{I} < Pt^{II}$, with $\Delta G^{\ddagger}$ (298.15 K) values ranging from 62 to 101 kJ mol^{-1}. The fluxions are sensitive only to the local metal-coordination environment, there being negligible electronic interaction between the metal centres in the dinuclear complexes. In the mixed-metal dinuclear complex $[ReBr(CO)_3PtIMe_3L^1]$ it proved possible to measure the different rates of fluxion of the Re^{I} and Pt^{IV} moieties.

2,2′:6′,2″-Terpyridine (terpy) has been studied for many years as a strong chelating agent to metals.[1] Its normal bonding mode to metals is a NNN terdentate ligand but towards certain types of kinetically inert metal moieties *e.g. fac*-$ReX(CO)_3$ it will act as a N,N bidentate chelate. In such bidentate complexes the ligand is fluxional and switches its metal coordination sites between adjacent pairs of its three nitrogen atoms by an associative mechanism.[2]

We are interested in studying the fluxional motions in metal complexes derived from nitrogen ligands that have the potential capability of binding more than one metal moiety in a bidentate chelate mode. We have reported[3] our studies of Pd^{II} and Pt^{II} complexes with the ligands 2,4,6-tris(2-pyridyl)-1,3,5-triazine (TPT) and 2,4,6-tris(2-pyridyl)pyrimidine (TPP) in which the fluxional processes of 1,4-metallotropic shift, metal-hurdling and restricted ring rotation were observed. We have now turned our attention to the study of metal complexes of N_6 ligands that are derived from linked subunits of terpy, each of which is capable of N,N bidentate or N,N,N terdentate chelation to a metal moiety.

We have used the ligands, 6,6″-bis(2-pyridyl)-2,2′:4′,4″:2″,2‴-quaterpyridine (L^1), 1,4-bis(2,2′:6′,2″-terpyridin-4-yl)-benzene (L^2), 6′,6″-bis{2-(4-methylpyridyl)}-2,2′:4′,4″:2″,2‴-quaterpyridine (L^3) to form the metal complexes $[\{ReBr(CO)_3\}_2L]$ (L = L^1, L^2 or L^3), $[(PtClMe_3)_2L^1]$, $[(PtIMe_3)_2L]$ (L = L^2 or L^3), $[ReBr(CO)_3L^1]$, $[Pt(C_6F_5)_2L^3]$, $[Pt(C_6F_4CF_3)_2L]$ (L = L^1 or L^2), $[\{Pt(C_6F_4CF_3)_2\}_2L]$ (L = L^1 or L^2) and $[ReBr(CO)_3PtIMe_3L^1]$, in all of which the ligands are acting in a bidentate chelate mode to the metal atom(s). We now report our dynamic NMR studies on these complexes.

Experimental

Materials

The compounds $[ReBr(CO)_5]$,[4] $[PtXMe_3]_4$[5] (X = Cl or I), $[Pt(C_6F_5)_2(diox)_2]$ (diox = 1,4-dioxane),[6] $[NiCl_2(Ph_3P)_2]$,[7] $[Pt(C_6F_4CF_3)_2(Et_2S)_2]$,[8] 4-methyl-4′-methylthio-2,2′:6′,2″-terpyridine,[9] 6′,6″-bis(2-pyridyl)-2,2′:4′,4″:2″,2‴-quaterpyridine[10] (L^1) and 1,4-bis(2,2′:6′,2″-terpyridin-4′-yl)benzene[10] (L^2) were prepared according to literature methods.

6′,6″-Bis{2-(4-methylpyridyl)}-2,2′:4′,4″:2″,2‴-quaterpyridine (L^3)

The complex $[NiCl_2(PPh_3)_2]$ (12.8 g, 19.5 mmol) and PPh_3 (10.3 g, 39.4 mmol) were added to dried and degassed dimethylformamide and stirred for 10 min to give a blue solution. Zinc dust (1.28 g, 19.2 mmol) was added and the resulting suspension stirred for 1 h, after which time the colour had changed from blue to red. 4-Methyl-4′-methylthio-2,2′:6′,2″-terpyridine (2.5 g, 8.5 mmol) was added and the resulting suspension stirred for 16 h causing the colour to change to a very dark green. The solvent was then removed *in vacuo*, and the resulting black tar was extracted with $CHCl_3$ (2 × 250 cm^3) to leave a brown solid which was dried and then added to aqueous ammonia (0.88 specific gravity, 400 cm^3) and stirred for 24 h. After this time the grey solid residue was collected by filtration, thoroughly dried and then extracted with $CHCl_3$ (450 cm^3). The green solution was dried ($MgSO_4$) and then concentrated in volume to *ca*. 40 cm^3, methanol (200 cm^3) was added and the resulting solution cooled (−20 °C) for 16 h. The cream solid that precipitated was collected and washed with methanol to yield the desired product as a cream solid. Yield 0.6 g (14%).

Synthesis of complexes

All preparations were carried out using standard Schlenk techniques[11] under purified nitrogen using freshly distilled and degassed solvents. Synthetic and analytical data are given in Table 1. In some cases difficulties were experienced in securing good analytical data due to persistent contamination with either free ligand, solvent or another metal complex.

2:1 Complexes. The complexes $[\{ReBr(CO)_3\}_2L]$ (L = L^1, L^2 or L^3), $[(PtClMe_3)_2L^1]$, $[(PtIMe_3)_2L]$ (L = L^2 or L^3) and $[\{Pt(C_6F_4CF_3)_2\}_2L]$ (L = L^1 or L^2) were all prepared in analogous manner from the reaction of the appropriate ligand with at least

Table 1 Synthetic and analytical data for mono- and di-nuclear Re^{I}, Pt^{II} and Pt^{IV} complexes of ligands L^1, L^2 and L^3

Complex	Yield	$\tilde{\nu}_{CO}$ or $\tilde{\nu}_{MC}$ [a]/cm^{-1}	Analysis [b] (%) C	H	N	*m*/*z*
$[\{ReBr(CO)_3\}_2L^1]$	40	2023s, 1920m, 1912sh [c]	35.8(37.1)	1.4(1.7)	6.4(7.2)	1164$[M]^+$
$[ReBr(CO)_3L^1]$	14	2025s, 1924m, 1901m [d]	[e]	[e]	[e]	—
$[(PtClMe_3)_2L^1]$	22	—	41.9(42.5)	4.1(3.7)	7.8(8.3)	979$[M - Cl]^+$
$[ReBr(CO)_3PtIMe_3L^1]$	61	2025s, 1924m, 1901m [d]	[f]	[f]	[f]	1182$[M + H]^+$
$[Pt(C_6F_4CF_3)_2L^1]$	42	790m, 711w	48.7(48.3)	2.0(1.8)	7.6(7.7)	—
$[\{Pt(C_6F_4CF_3)_2\}_2L^1]$	88	791m, 711s	41.7(40.4)	1.6(1.2)	6.1(4.9)	—
$[Pt(C_6F_4CF_3)_2L^2]$	28	792m, 711s	[g]	[g]	[g]	—
$[\{Pt(C_6F_4CF_3)_2\}_2L^2]$	73	790m, 713s	42.1(42.7)	2.4(1.3)	4.3(4.7)	—
$[\{ReBr(CO)_3\}_2L^2]$	35	2021s, 1912m, 1890sh [h]	39.8(40.6)	2.2(1.9)	6.2(6.8)	1241$[M + H]^+$
$[(PtIMe_3)_2L^2]$	36	—	39.0(39.8)	2.2(2.6)	6.0(6.6)	—
$[\{ReBr(CO)_3\}_2L^3]$	73	2024s, 1921m, 1900sh [d]	38.1(38.3)	2.0(2.0)	6.6(7.0)	1193$[M + H]^+$
$[(PtIMe_3)_2L^3]$	31	—	36.8(37.2)	3.3(3.4)	6.4(6.9)	1099$[M - I]^+$
$[Pt(C_6F_5)_2L^3]$	20	—	51.0(51.7)	2.2(2.4)	7.9(8.2)	—

[a] s = strong, m = medium, sh = shoulder. [b] Calculated values in parentheses. [c] Recorded in benzene solution. [d] Recorded in CH_2Cl_2 solution. [e] Analytically pure samples could not be produced due to persistent contamination with $[\{ReBr(CO)_3\}_2L^1]$. [f] Analytically pure samples could not be produced due to difficulty in obtaining a pure sample of $[ReBr(CO)_3L^1]$. [g] Analytically pure samples could not be produced due to persistent contamination with L^2. [h] Recorded in THF solution.

2 molar equivalents of the corresponding metal halide or Et_2S complex. The preparation of the complex $[\{ReBr(CO)_3\}_2L^1]$ is described in more detail below by way of illustration.

Bis{bromotricarbonylrhenium(I)}μ,η⁴-{6′,6″-bis(2-pyridyl)-2,2′:4′,4″:2″,2‴-quaterpyridine}. The compound $[ReBr(CO)_5]$ (0.2 g, 0.49 mmol) and L^1 (0.1 g, 0.22 mmol) were dissolved in benzene (80 cm^3) and the resulting solution heated under reflux for 16 h, after which time the solvent was concentrated to *ca*. 20 cm^3 and light petroleum (bp 40–60 °C, 100 cm^3) added to precipitate an orange solid. This solid was isolated, washed thoroughly with light petroleum (2 × 150 cm^3) and recrystallized from CH_2Cl_2–hexane to give the desired product as an orange powder. Yield 0.1 g (40%).

1:1 Complexes. The complexes $[Pt(C_6F_5)_2L^3]$ and $[Pt(C_6F_4CF_3)_2L]$ (L = L^1 or L^2) were prepared by the reaction of the ligand with approximately 1.5 molar equivalents of $[Pt(C_6F_5)_2(diox)_2]$ or $[Pt(C_6F_4CF_3)_2(Et_2S)_2]$. The complex $[ReBr(CO)_3L^1]$ was found to be extremely difficult to obtain free from contamination with ligand L^1 or the complex $[\{ReBr(CO)_3\}_2L^1]$. The preparations for two complexes are described as examples.

cis-Bis(pentafluorophenyl)[6′,6″-bis{2-(4-methylpyridyl)}-2,2′:4′,4″:2″,2‴-quaterpyridine]platinum(II). The compounds *trans*-$[Pt(C_6F_5)_2(diox)_2]$ (0.17 g, 0.27 mmol) and L^3 (0.085 g, 0.17 mmol) were dissolved in benzene (50 cm^3) and the resulting solution heated under reflux for 16 h. After this time the volume was reduced to *ca*. 15 cm^3 and light petroleum (bp 40–60 °C, 120 cm^3) added to precipitate a yellow solid. This solid was extracted with ice-cold tetrahydrofuran (3 × 10 cm^3), hexane (80 cm^3) was added and the resulting solution cooled (at −20 °C) for 16 h to produce the desired product as a red solid. Yield 0.035 g (20%).

Bromotricarbonyl{6′,6″-bis(2-pyridyl)-2,2′:4′,4″:2″,2‴-quaterpyridine}rhenium(I). A solution of $[ReBr(CO)_3(THF)_2]$ [prepared from $[ReBr(CO)_5]$ (0.1 g, 0.26 mmol) heated under reflux in tetrahydrofuran (20 cm^3) for 12 h] was diluted with hexane (120 cm^3) and added dropwise over 1.5 h to a stirred solution of L^1 (0.2 g, 0.43 mmol) in a mixture of chloroform and hexane (120:85 cm^3) at −70 °C. The temperature was allowed to rise to −20 °C and hexane (500 cm^3) added to produce a yellow precipitate which was isolated by filtration. The solid was extracted with ice-cold tetrahydrofuran (2 × 15 cm^3) and hexane (100 cm^3) added to yield an orange precipitate which was isolated and dried under vacuum, to give the desired product as an orange solid. Yield 0.03 g (14%). [The cold extraction was designed to remove the 1:1 complex from the less soluble unreacted ligand and as such was reasonably successful, as the ^{1}H NMR spectrum indicated the presence of *ca*. 3% unreacted ligand which could not be removed by further extractions.]

Mixed metal complex. *Bromotricarbonylrhenium(I)μ,η⁴-{6′,6″-bis(2-pyridyl)-2,2′:4′,4″:2″,2‴-quaterpyridine}iodotrimethylplatinum(IV)*. A solution of $[PtIMe_3]_4$ (0.042 g, 0.15 mmol) heated under reflux in tetrahydrofuran (65 cm^3) for 16 h was added to a solution of $[ReBr(CO)_3L^1]$ (0.09 g, 0.11 mmol) in tetrahydrofuran (20 cm^3) and the resulting orange solution stirred at 45 °C for 4 h. After this time the colour of the solution had changed to cherry red. The volume was reduced to *ca*. 30 cm^3 and hexane (100 cm^3) added to produce an orange precipitate which was isolated and dried under vacuum to yield the desired product. Yield 0.08 g (61%).

Physical methods

Hydrogen-1 NMR spectra were recorded on either Bruker AC-300 or DRX-400 spectrometers operating at 300.13 or 400.13 MHz respectively. ^{19}F NMR spectra were also recorded on the DRX-400 spectrometer operating at 376.46 MHz. All chemical shifts are quoted relative to either $SiMe_4$ (^{1}H) or C_6F_6 (^{19}F) ($\delta = 0$) respectively. Variable temperature NMR spectra were obtained using the Bruker variable temperature units B-VT 1000 (AC300) and B-VT 2000 (DRX-400) to control the probe temperature, calibration being periodically checked against a Comark digital thermometer. Sample temperatures are considered accurate to ±1 °C. The ^{195}Pt spectrum of complex $[(PtIMe_3)_2L^3]$ was recorded as a $(CDCl_2)_2$ solution at 273 K using a Bruker DRX-400 spectrometer operating at 85.63 MHz with ^{195}Pt shifts quoted relative to $\Xi(^{195}Pt) = 21.4$ MHz. Two-dimensional exchange (EXSY) spectra and homonuclear correlated (COSY) spectra were obtained using the standard Bruker programs NOESYPH.AU and COSY.AU respectively. Mixing times in the EXSY experiments were chosen in the range 0.5–1.5 s according to the nature of the complex and the temperature of measurement. Rate data were derived from bandshape analysis of the ^{1}H spectra using a version of the DNMR3 program,[12] or from 2D-EXSY spectra using volume integration data in the authors D2DNMR program.[13] Activation parameters based on experimental rate data were calculated using the THERMO program.[14]

Infrared spectra were recorded on a Perkin-Elmer 881 spectrometer calibrated from the signal of polystyrene at 1602 cm^{-1}. Elemental analyses were performed by Butterworth Laboratories, Teddington, Middlesex, London.

Electron impact mass spectra were measured on a Kratos

Table 2 ^{1}H NMR data for the ligand L^1 and its dinuclear complexes $[M_2L^1]$ {M = $ReBr(CO)_3$, $PtClMe_3$ or $Pt(C_6F_4CF_3)_2$}

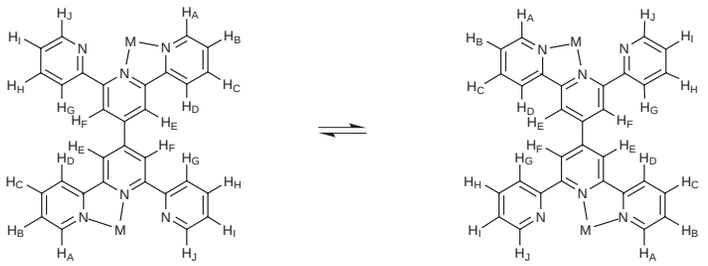

Compound	Solvent	T/K	δ_{AJ}	δ_{BI}	δ_{CH}	δ_{DG}	δ_{EF}	δ_{Me} [a]
L^1	$CDCl_3$	303	8.76	7.38	7.90	8.70	8.97	
$[\{ReBr(CO)_3\}_2L^1]$	$(CD_3)_2SO$	303	9.09(A)	7.78(B)	8.36(C)	9.06(D)	9.36(E)	
			8.79(J)	7.63(I)	8.06(H)	7.90(G) [b]	8.63(F) [b]	
$[(PtClMe_3)_2L^1]$	CD_3NO_2	273	8.94(A)	7.83(B)	8.30(C)	8.72(D)	9.02(E)	1.30(A)(74.7)
			8.75(J)	7.56(I)	7.95(H)	8.51(G)	8.61(F)	0.08(B)(73.4)
								0.34(C)(77.4)
$[\{Pt(C_6F_4CF_3)_2\}_2L^1]$	$(CDCl_2)_2$	303	8.48(A)	7.67(B)	8.34(C)	8.40(D)	8.66(E)	
			8.52(J)	7.28(I)	7.84(H)	8.11(G)	8.46(F)	

[a] Pt–Me shifts, $^2J_{PtH}$/Hz values in parentheses, Me_C axial, $Me_{A,B}$ equatorial. [b] Signals further split due to two rotameric forms of the pendant pyridyl rings.

Profile spectrometer in this Department and FAB mass spectra obtained on a VG AutoSpec instrument (Cs^+ bombardment) at the University of Wales, Swansea.

Results

The solution NMR properties of the three 'back-to-back' terpy ligands L^1, L^2 and L^3 and their metal coordination complexes (both 2:1 and 1:1 metal:ligand ratios) will be described in turn, with the high and low temperature studies discussed separately.

Ambient and high temperature NMR spectra

Ligand L^1 and its dinuclear complexes $[M_2L^1]$ {M = $ReBr(CO)_3$, $PtClMe_3$ or $Pt(C_6F_4CF_3)_2$}. The ambient temperature ^{1}H NMR data of these compounds are collected in Table 2. The free ligand gives rise to five equal-intensity chemical shifts with values similar to terpy itself. The main difference concerns the central pyridyl signals H_E/H_F which are significantly deshielded compared to terpy. Ligand L^1 is depicted as a planar species with transoid arrangements of its pyridyl rings since 4-phenyl-2,2′:6′,2″-terpyridine is known to be planar in the solid state.[1] In solution rapid rotation is most likely to be occurring with its planar structures being the most favoured conformations. Such conformations account for the considerable deshielding of the central pyridyl H_E/H_F signals by the ring currents of the adjacent rings. If the two terpy units of the ligand were not rotating relative to each other but were locked at some angle, then the deshielding effects of the central pyridyl hydrogens could not be easily explained.

The spectra of the 2:1 metal:ligand complexes comprise 10 aromatic signals at ambient temperatures arising from the reduced symmetry of the complexes compared to the free ligands. Chemical environments are labelled A–J and shifts assigned as in Table 2. The observed number of chemical shifts implies essentially free rotation in the ligand about the C–C bond linking the two central pyridyl rings causing there to be no relative positional dependence of metal coordination on the two sides of the ligand. For the Re^I and Pt^{IV} complexes the coordination shifts are mainly positive, particularly for H_A which is just three bonds removed from the metal centre. For the Pt^{II} complex a mixture of positive and negative coordination shifts occur with the H_A shift being significantly negative. This has been noted previously[15] in the case of terpy complexes

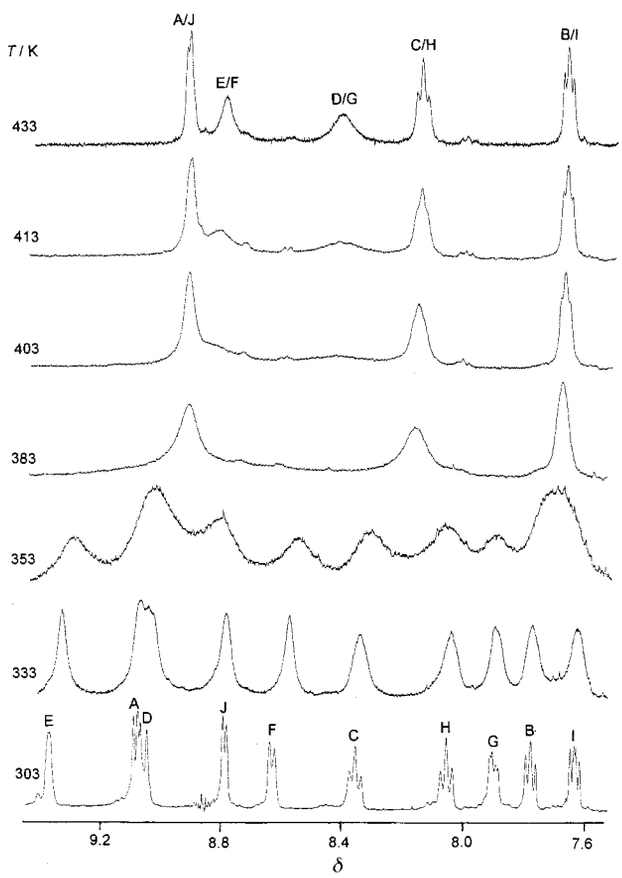

Fig. 1 Variable temperature 400 MHz ^{1}H NMR spectra of $[\{ReBr(CO)_3\}_2L^1]$ in $(CD_3)_2SO$ showing the effects of 1,4-metallotropic shifts. The signal labelling refers to Table 2. Note the additional splitting of signals F and G due to rotameric distinction.

and is attributed to the shielding of the adjacent $C_6F_4CF_3$ ring which adopts a near-orthogonal orientation with respect to the coordinated pyridyl rings.

The ^{1}H NMR spectra of $[\{ReBr(CO)_3\}_2L^1]$ in $(CD_3)_2SO$ at ambient and various above-ambient temperatures are shown in Fig. 1. The signals show the expected multiplet splittings due to three-bond scalar couplings, but signals due to H_F and H_G show further splittings into unequal intensity doublets (relative inten-

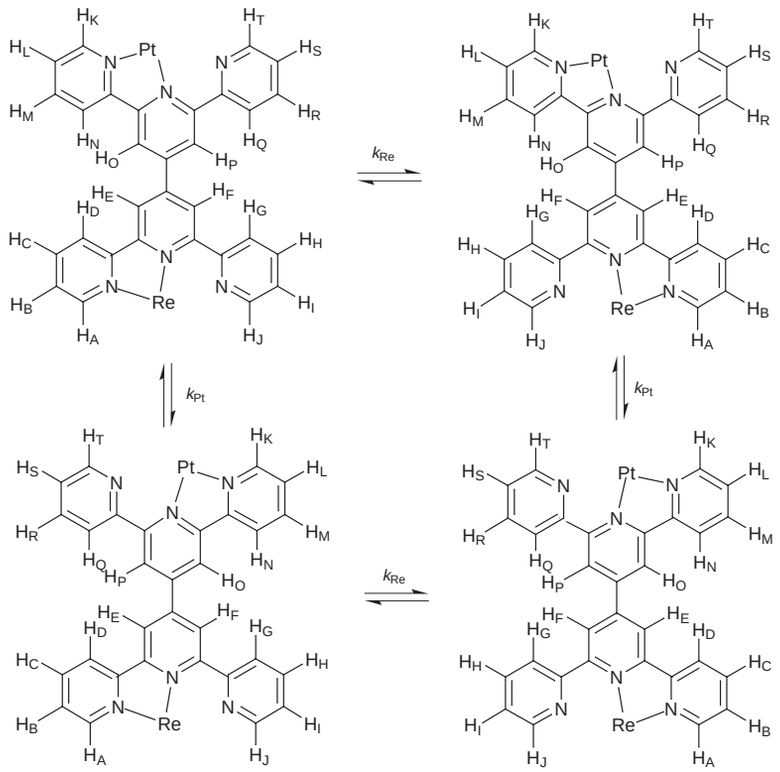

Fig. 2 Interconversion of the four equivalent structures of $[ReBr(CO)_3PtIMe_3L^1]$ as a result of the Re^I and Pt^{IV} moiety M–N shifts. The chemical shifts of the exchanging pairs of signals are measured at 253 K in $(CDCl_2)_2$ solvent. The asterisks refer to the pairs of signals used for bandshape analysis.

sities 55:45%). This splitting soon vanished on warming and is attributed to restricted rotation of the pendant pyridyl rings. At 303 K two distinct rotameric species occur which differ in their orientations with respect to the central pyridyl ring, and with one rotamer being rotated, by approximately 180°, with respect to the other rotamer. The environments of H_F and H_G are most sensitive to these different rotameric species. On warming the solution of the complex all bands commence broadening with pairs of bands coalescing and sharpening at different rates. By 433 K the spectrum consists of five averaged bands of differing widths, due to the exchanges A ⇌ J, B ⇌ I, C ⇌ H, D ⇌ G and E ⇌ F which have occurred as a result of the 1,4-metallotropic shifts of either metal moiety. Rates of these fluxions were measured by bandshape analysis of the exchanging B and I signals, taking account of the multiplet splittings of the three-bond scalar couplings. Spectra at nine different temperatures were fitted and reliable activation energy data obtained (see later).

The variable temperature ^1H spectra of $[(PtClMe_3)_2L^1]$ showed very analogous changes. Spectra were recorded in CD_3NO_2 solvent in the range 263 to 368 K and the bandshapes of the exchanging B and I signals fitted at ten different temperatures.

The variable temperature ^1H NMR spectra of the mixed-metal dinuclear complex $[ReBr(CO)_3PtIMe_3L^1]$ were more challenging to interpret. Fluxional shifts of either metal moiety leads to exchange between the four structural species shown in Fig. 2. Assuming unrestricted rotation about the central C–C bond linking the two terpy ligands, all four species are chemically identical but two different rates of fluxion will occur depending on which metal moiety moves. These can be distinguished by NMR as they lead to different averagings of the aromatic hydrogen environments. These different averagings are

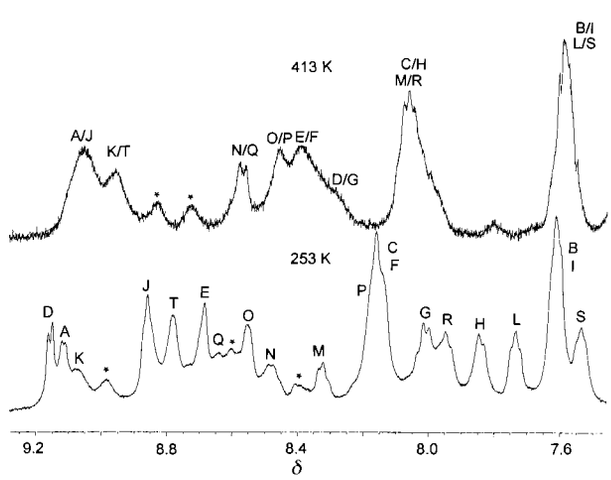

Fig. 3 400 MHz ^1H spectra of $[ReBr(CO)_3PtIMe_3L^1]$ in $(CDCl_2)_2$ measured at 253 and 413 K. The asterisks denote impurity bands of $[\{ReBr(CO)_3\}_2L^1]$. See Fig. 2 for signal labelling.

Table 3 ^{1}H NMR data for the ligand L^1 and its complexes $[ReBr(CO)_3L^1]$ and $[Pt(C_6F_4CF_3)_2L^1]$ at 303 K

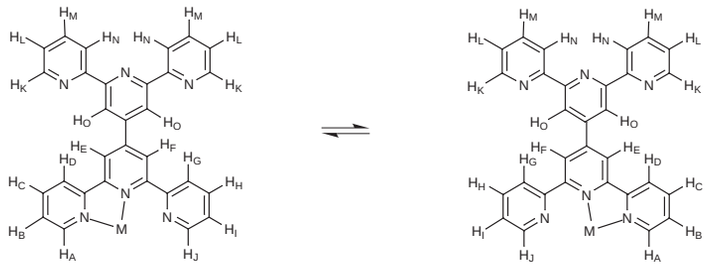

Compound	Solvent	δ_{AJK}	δ_{BIL}	δ_{CHM}	δ_{DGN}	δ_{EFO}
L^1	$CDCl_3$	8.76	7.38	7.90	8.70	8.97
$[ReBr(CO)_3L^1]$	$(CDCl_2)_2$	9.15(A)	7.62(B)	8.19(C)	8.57(D)	8.75(E)
		8.90(J)	7.60(I)	8.04(H)	7.94(G)	8.26(F)
		8.77(K)	7.45(L)	7.98(M)	8.74(N)	8.91(O)
$[Pt(C_6F_4CF_3)_2L^1]$	$CDCl_3$	8.38(A)	7.58(B)	8.28(C)	8.48(D)	8.67(E)
		8.52(J)	7.20(I)	7.71(H)	7.91(G)	8.45(F)
		8.76(K)	7.44(L)	7.95(M)	8.72(N)	8.92(O)

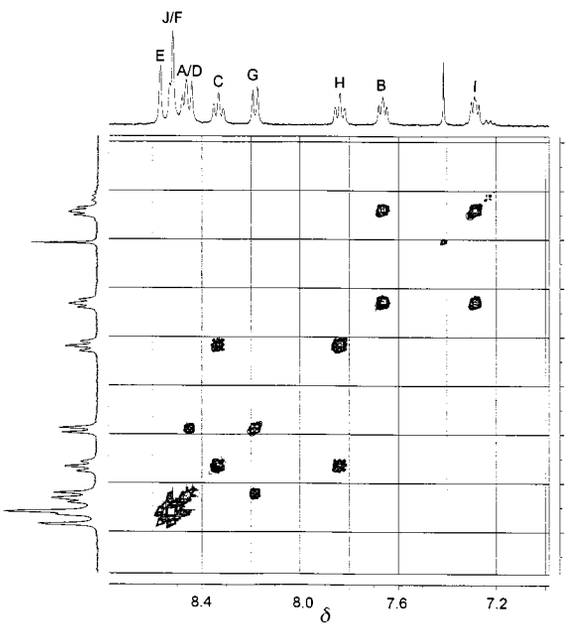

Fig. 4 400 MHz ^{1}H 2D-EXSY NMR spectrum of $[\{Pt(C_6F_4CF_3)_2\}_2L^1]$ in $(CDCl_2)_2$ at 393 K. Mixing time was 0.8 s. Signal labelling refers to Table 2.

listed in Fig. 2 together with chemical shifts measured at 253 K in $(CDCl_2)_2$ solvent. The spectrum at this temperature is shown in Fig. 3. The metal fluxions are slow on the ^{1}H chemical shift time scale at this temperature, but are slightly broadened by restricted rotations of the pendant pyridyl rings. The assignment of the 20 signals is fairly firm as a result of careful comparison with the previous spectra of the like-metal moiety analogues. On warming the $(CDCl_2)_2$ solution of the complex numerous bandshape changes occurred as a result of the onset of the fluxions of both metal moieties. By 413 K, the high temperature limit of the solvent, the spectra had simplified to 10 averaged signals, two pairs of which had very similar chemical shifts. The signals still displayed varying amounts of exchange broadening and little multiplet structure could be detected. The spectra were too complex for bandshape analysis to be performed but estimates of fluxional rates of both metal moieties were made from the coalescence temperatures of the appropriate exchanging signals, namely coalescence of signals L and S at 323 K as a result of $PtIMe_3$ fluxion and coalescence of signals A and J at 353 K resulting from $ReBr(CO)_3$ fluxion.

The ^{1}H spectra of $[\{Pt(C_6F_4CF_3)_2\}_2L^1]$ were essentially temperature independent in the range ambient to 393 K indicating stereochemical rigidity. It was therefore apparent that no reliable kinetic data would be obtainable without recourse to 2D-exchange spectroscopy (2D-EXSY). Accordingly, a ^{1}H 2D-EXSY spectrum was obtained at 393 K (Fig. 4). Using a mixing time of 0.8 s, cross peaks between the exchanging pairs B ⇌ I, C ⇌ H and D ⇌ G were clearly detected indicating that the 1,4-metallotropic shift was indeed proceeding albeit at a slow rate. Relative intensities of the diagonal and cross peaks of the above signals were measured and used as input into the D2DNMR program.[13] Three sets of rate constants were computed, and an average value used to estimate the Gibbs free energy of activation of the process using the Eyring equation.

Mononuclear complexes $[ReBr(CO)_3L^1]$ and $[Pt(C_6F_4CF_3)_2L^1]$. The synthesis of $[ReBr(CO)_3L^1]$ was difficult as the reaction preferentially proceeded to the dinuclear complex. However, its ^{1}H chemical shifts were measured and assigned (Table 3). The uncoordinated half of the ligand gave rise to five chemical shifts (due to the environments K–O), indicating rapid rotation about the C–C bond linking the two halves of the ligand. If the two halves were locked at some angle then the symmetry of the *fac*-$ReBr(CO)_3$ moiety with its differing axial groups would remove the chemical equivalence of the two outer pyridyl rings on the uncoordinated side, and this was not observed.

Coordination shifts of the aromatic hydrogens on the coordinated side of the complex are very similar to those of the dinuclear Re complex, whilst the chemical shifts on the uncoordinated side are very similar to those of the free ligand L^1. On warming, the spectra changed in the predicted way, coalescences occurring between the signal pairs A ⇌ J, B ⇌ I, C ⇌ H, D ⇌ G and E ⇌ F. The signals K, L, M, N and O remained sharp at all temperatures. Bandshape analysis was performed on the A ⇌ J exchanging pair, spectra at 11 temperatures in the range 303–413 K being fitted. The spectra also showed traces of free ligand but these did not affect the accuracy of the NMR analyses.

The ^{1}H spectra of $[Pt(C_6F_4CF_3)_2L^1]$ were essentially unchanged on heating the solution to *ca.* 393 K. As in the case of its dinuclear analogue, a 2D-EXSY spectrum was taken at 393 K (Fig. 5) and again it revealed slow fluxional exchange. In this case all five expected pairs of cross peaks were detected. The exchanging pairs B ⇌ I and C ⇌ H were chosen for the rate constant calculations. No cross peaks were detected between signals K–O as these are unaffected by the Pt^{II} fluxions.

Table 4 ^{1}H NMR data for the ligand L^2 and its dinuclear complexes

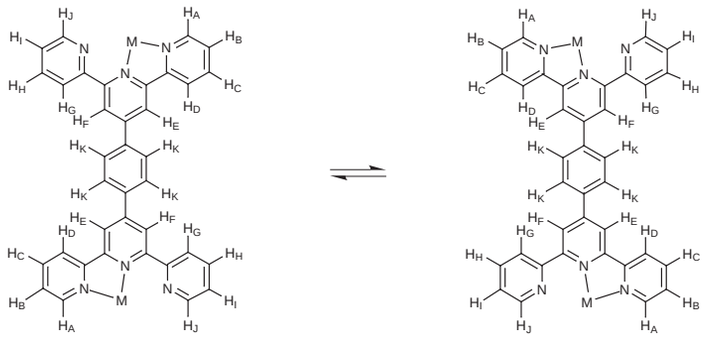

Compound	Solvent	T/K	δ_{AJ}	δ_{BI}	δ_{CH}	δ_{DG}	δ_{EF}	δ_{K}	δ_{Me} [a]
L^2	$CDCl_3$	303	8.77	7.38	7.90	8.71	8.83	8.08	—
$[\{ReBr(CO)_3\}_2L^2]$	$(CDCl_2)_2$	303	9.16(A)	7.61(B)	8.18(C)	8.46(D)	8.51(E)	8.02	—
			8.89(J)	7.61(I)	8.02(H)	7.91(G)	8.04(F)		
$[(PtIMe_3)_2L^2]$	$CDCl_2)_2$	253	9.03(A)	7.68(B)	8.14(C)	8.37(D)	8.42(E)	7.99	1.62(A)(74.2)
			8.74(J)	7.47(I)	7.89(H)	8.55(G) [b]	8.17(F)		0.34(B)(69.4)
									0.55(C)(68.6)
$[\{Pt(C_6F_4CF_3)_2\}_2L^2]$	$(CDCl_2)_2$	303	8.35(A)	7.62(B)	8.29(C)	8.40(D)	8.47(E)	8.11	
			8.49(J)	7.24(I)	7.76(H)	8.00(G)	8.31(F)		

[a] Pt–Me shifts, $^2J_{PtH}$/Hz values in parentheses, Me_C axial, $Me_{A,B}$ equatorial. [b] Broad band.

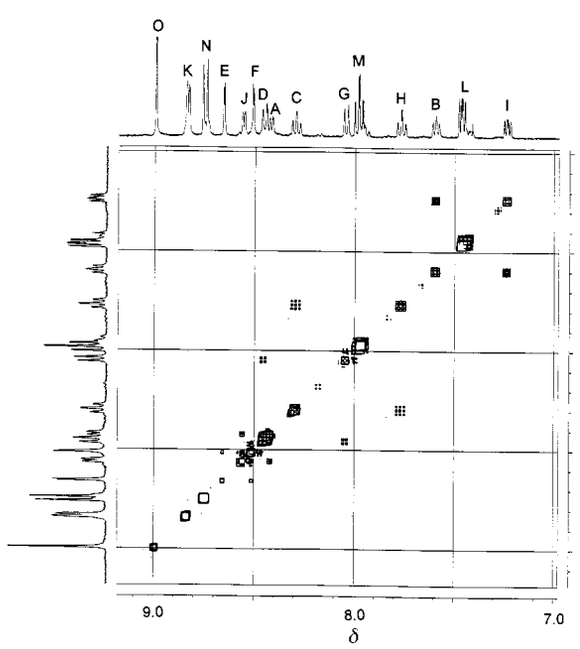

Fig. 5 400 MHz ^{1}H 2D-EXSY NMR spectrum of $[Pt(C_6F_4CF_3)_2L^1]$ in $(CDCl_2)_2$ at 393 K. Mixing time was 0.8 s. Signal labelling refers to Table 3.

Ligand L^2 and its dinuclear complexes $[M_2L^2]$ {M = ReBr(CO)$_3$, PtIMe$_3$ or Pt(C$_6$F$_4$CF$_3$)$_2$}. The ^{1}H spectrum of the free ligand L^2 was straightforwardly assigned (Table 4). The hydrogens of the central phenyl 'spacer' ring produced a sharp singlet indicative of free rotation with respect to the attached pyridyl rings. The Re^I, Pt^{IV} and Pt^{II} complexes of L^2 gave very analogous spectra to the corresponding L^1 analogues. Their spectra also changed with temperature in analogous ways. The fluxional rates of the $ReBr(CO)_3$ and $PtIMe_3$ moieties became fast on the NMR timescale by 413 K, and bandshape analyses were performed with accuracy. Spectra at 11 different temperatures were fitted in the temperature range 273–413 K, signals A/J being used for the Re^I complex and signals B/I for the Pt^{IV} complex. The fluxion of $[\{Pt(C_6F_4CF_3)_2\}_2L^2]$ was again very much slower and could only be revealed by 2D-EXSY experiments at elevated temperatures.

Mononuclear complex $[Pt(C_6F_4CF_3)_2L^2]$. The static ^{1}H spectral data of this complex are given in Table 5. They consist of 17 chemical shifts all of which have been assigned with confidence. The signals of the central phenyl ring comprise an AA′BB′ spin system although the cross ring couplings are only just resolved. The fluxion of the Pt^{II} moiety was again revealed in a high temperature 2D-EXSY spectrum (413 K, mixing time 0.8 s). The dynamic process had no effect on the signals K–Q (see Table 5 for labelling).

Ligand L^3 and its complexes $[(PtIMe_3)_2L^3]$ and $[Pt(C_6F_5)_2L^3]$. Our recent investigation[2] into the mechanism of the 1,4-metallotropic shift in bidentate chelate complexes required the preparation of complexes of unsymmetrically substituted terpyridine ligands. We have now utilized the synthetic route to such ligands to prepare unsymmetrical back-to-back terpy ligands such as ligand L^3. The ^{1}H NMR spectrum of this compound consists of nine aromatic hydrogen signals and one methyl signal, which imply rapid rotation about the central C–C bond causing chemical equivalence of both terpy fragments (Table 6).

This ligand is capable of forming more than one chemically distinct type of dinuclear or mononuclear complex and these were examined in detail below.

The dinuclear complex $[(PtIMe_3)_2L^3]$ gave a broad, ill-defined ^{1}H spectrum at room temperature, which became better resolved on cooling to 253 K. This is shown in Fig. 6. Some of the bands are still somewhat broadened but this was attributed to the effects of restricted rotation of the pendant rings. The unsymmetrical nature of the complex presents the possibility of chemically distinct metal complexes according to whether coordination involves the 4-methylpyridyl ring or not. Previous studies[2] on the complexes $[M(C_6F_5)_2(mcpt)]$ [M = Pd^{II} or Pt^{II}, mcpt = 4-methyl-4′-(4-chlorophenyl)-2,2′ : 6′,2″-terpyridine] have shown that coordination involving the N-heteroatom of a 4-methylpyridyl ring is slightly preferred over the unsubstituted ring. Thus, the most preferred coordination complex of $[(PtIMe_3)_2L^3]$ will involve coordination of both 4-methylpyridyl rings. This structure is labelled major/major in Fig. 7 and is one of a set of four. A metallotropic shift of either Pt moiety will lead to a mixed 4-methylpyridyl/pyridyl ring coordinated species (major/minor or minor/major, Fig. 7). A further fluxional shift will produce a species where neither 4-methylpyridyl

Table 5 ^{1}H NMR data for the ligand L^2 and its mononuclear metal complex $[Pt(C_6F_4CF_3)_2L^2]$

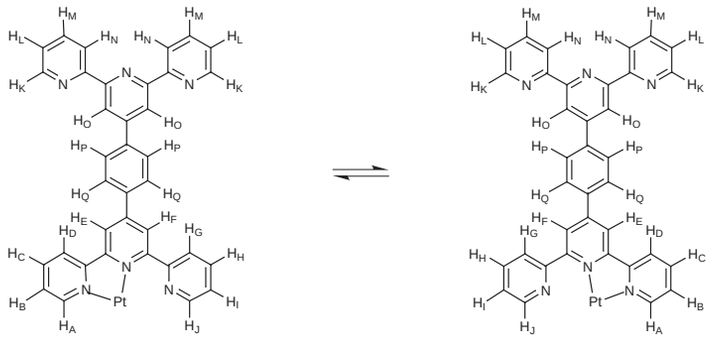

Compound	Solvent	T/K	δ_{AJK}	δ_{BIL}	δ_{CHM}	δ_{DGN}	δ_{EFO}	δ_{PQ}
L^2	$CDCl_3$	303	8.77	7.38	7.90	8.71	8.83	8.08
$[Pt(C_6F_4CF_3)_2L^2]$	$CDCl_3$	303	8.36(A)	7.54(B)	8.23(C)	8.36(D)	8.41(E)	8.04(P)
			8.49(J)	7.18(I)	7.70(H)	7.96(G)	8.23(F)	8.11(Q)
			8.74(K)	7.38(L)	7.91(M)	8.70(N)	8.78(O)	

Table 6 ^{1}H NMR data[a] for ligand L^3 and its mono- and di-nuclear complexes

Compound	Solvent	T/K	δ_{AT}	δ_{BS}	δ_{CR}	δ_{DQ}	δ_{EP}	δ_{FO}	δ_{GN}	δ_{HM}	δ_{IL}	δ_{JK}	Notes
L^3	$CDCl_3$	303	8.58	7.15	2.47	8.46	8.92	8.92	8.66	7.87	7.34	8.73	
$[(PtIMe_3)_2L^3]$	$(CDCl_2)_2$	253	8.90(A)	7.55(B)	2.64(C)	8.26(D)	8.60(E)	8.35(F)	8.75(G)	7.95(H)	7.55(I)	8.80(J)	[b]
			8.63(T)	7.34(S)	2.52(R)	8.60(Q)	8.46(P)	8.42(O)	8.49(N)	8.19(M)	7.74(L)	9.12(K)	[b]
$[Pt(C_6F_5)_2L^3]$	$(CDCl_2)_2$	353	8.25(A)	7.35(B)	2.60(C)	8.24(D)	8.62(E)	8.45(F)	8.06(G)	7.74(H)	7.23(I)	8.55(J)	[c]
			8.42(T)	7.05(S)	2.47(R)	7.85(Q)	8.45(P)	8.64(O)	8.45(N)	8.27(M)	7.55(L)	8.45(K)	[c]
			8.67	7.29	2.60	8.55	8.96	8.96	8.75	8.00	7.47	8.82	[d]

[a] See Fig. 7 for labelling. [b] Additional data: δ_{Me}, major signals 1.65(A)(74.0), 0.32(B)(68.0), ≈0.45(C), minor signals 1.68(A)(72), 0.37(B)(70.0), ≈0.45(C). $^2J_{PtH}$/Hz values in parentheses, C axial methyls (signals broadened due to restricted rotation of pendant ring), A,B equatorial methyls. ^{195}Pt shifts (273 K), rel. to $\Xi(^{195}Pt) = 21.4$ MHz, 1870.9(major), 1874.3(minor). [c] Data refer to coordinated side of ligand. [d] Data refer to uncoordinated side of ligand and to corresponding nuclei in the free ligand (see first row of table).

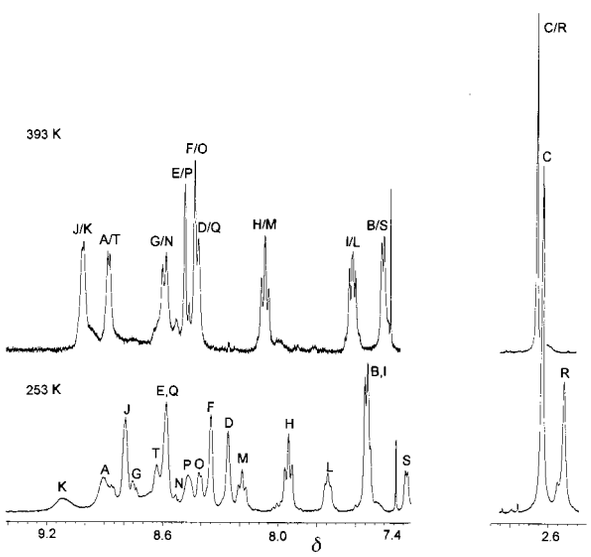

Fig. 6 400 MHz ^{1}H NMR spectrum of $[(PtIMe_3)_2L^3]$ in $(CDCl_2)_2$ at 253 and 393 K, the slow and fast exchange limits of Pt–N metallotropic shifts. Signal labelling refers to Table 6.

ring is coordinated (the minor/minor species, Fig. 7). These four structures constitute three chemically distinct types, but only two are NMR-distinguishable species, since the NMR shifts (^{1}H or ^{195}Pt) relate only to individual halves of the complexes, there being no magnetic influence between the two halves. Thus the ^{1}H shifts represent the summations of the hydrogen environments A–J on the 4-methylpyridyl-coordinated sides of the major/major, major/minor and minor/major complexes and of the hydrogen environments K–T on the pyridyl-coordinated sides of the major/minor, minor/major and minor/minor complexes, Fig. 7. These two sets of signals observed in the ^{1}H spectrum at 253 K (Fig. 6) are in the intensity ratio 64 : 36%, which leads to the four static structures having solution populations of (64/4) × 2 = 32% (major/major), (64/4) + (36/4) = 25% (major/minor), (36/4) + (64/4) = 25% (minor/major) and (36/4) × 2 = 18% (minor/minor). By careful comparison with previous related spectra, knowledge of the expected coordination shifts of the Pt^{IV} moiety and a close examination of the higher temperature spectra (Fig. 6) a fairly definitive assignment of all 20 lines was made (Table 6). The onset of metallotropic shifts of either Pt^{IV} moiety led to exchange broadening, coalescence and eventual sharpening of the averaged bands of ten pairs of signals. A fast exchange spectrum was obtained at 393 K from which firm assignments were made (Fig. 6). The effects of the metallotropic shifts were seen most clearly in the methyl signals C and R and in the aromatic hydrogen signals H and M. From the coalescence of the latter pair at 313 K, an estimate of the free energy of activation for the fluxion was made.

Variable temperature ^{1}H spectra of the dinuclear complex $[\{ReBr(CO)_3\}_2L^3]$ were recorded but these proved very intractable and no definitive assignments could be made. On warming to 393 K, the spectra did appear to simplify to nine averaged aromatic signals and one methyl signal as expected for fluxional shifts of both Re^I moieties, but no estimates of fluxional rates were made.

The spectra of the mononuclear complex $[Pt(C_6F_5)_2L^3]$ were more tractable. They did not change with temperature in the range ambient to 393 K, and consisted of 27 aromatic signals and three methyl signals. Chemical shifts were measured at 353 K (Table 6) and firm assignments of all signals made on the basis of the free ligand spectrum, predicted coordination shifts, and a COSY spectrum at this elevated temperature (Fig. 8). A 2D-EXSY spectrum was then recorded at 393 K and showed

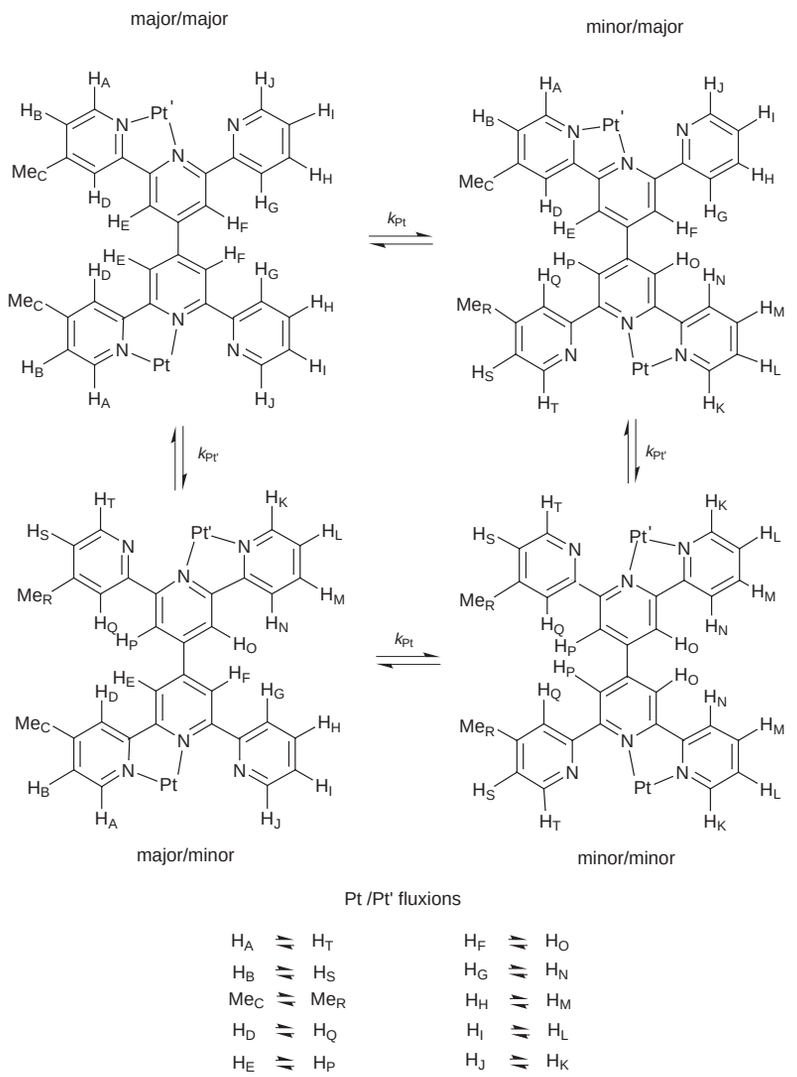

Fig. 7 Interconversion of the four structures of $[(PtIMe_3)_2L^3]$ following Pt^{IV} moiety fluxions.

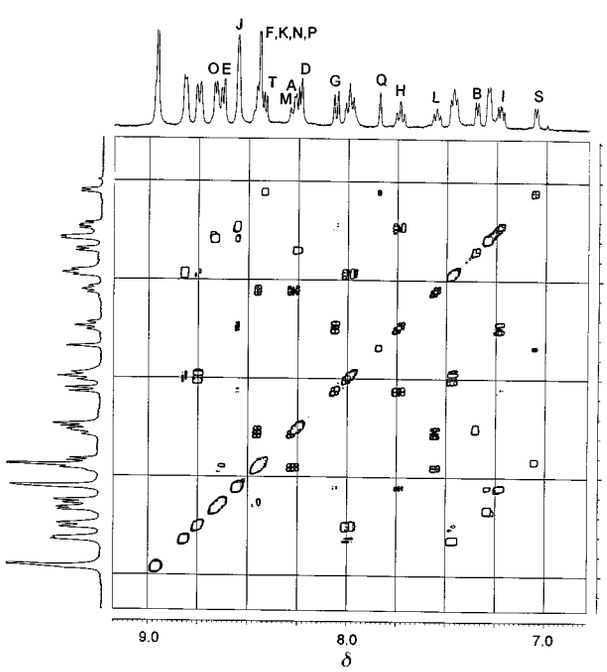

Fig. 8 400 MHz ^{1}H 2D-COSY45 NMR spectrum of $[Pt(C_6F_5)_2L^3]$ in $(CDCl_2)_2$ at 353 K. Labelling refers to Table 6 and Fig. 7. The unlabelled signals are due to hydrogens on the un-coordinated side of the ligand.

strong cross-peaks due to the following exchanges B ⇌ S, D ⇌ Q, G ⇌ N, H ⇌ M and I ⇌ L. The other changes expected as a result of the 1,4-metallotropic shift, namely A ⇌ T, E ⇌ P and F ⇌ O were present but somewhat obscured by signal overlaps. All signals of the uncoordinated terpy fragment were not associated with any exchange cross peaks. An estimate was made of the rate of the fluxional process at 393 K by measuring volume integrals of the diagonal and cross-peaks associated with the B ⇌ S and H ⇌ M exchanges, and using them as input data in the D2DNMR program.[13]

Low temperature NMR spectra

The Pt^{II} complexes of ligand L^1 and L^2 were also subjected to low temperature NMR study with a view to examining the rotational behaviour of the pendant pyridyl rings. It has been shown previously with the complexes $[M(C_6F_5)_2(terpy)]$ (M = Pd^{II}, Pt^{II})[15] and $[M(C_6F_4CF_3)_2(TPT)]$ [M = Pd^{II}, Pt^{II}, TPT = 2,4,6-tris(2-pyridyl)-1,3,5-triazine][3] that the *ortho* and *meta* ring fluorine nuclei of the perfluoroaromatic rings act as sensitive probes of the rates of pyridyl rotation. The perfluoroaromatic rings do not rotate with respect to the ^{19}F chemical shift time scale at below-ambient temperatures and so the *ortho* and *meta* ring fluorine signals broaden on cooling, and eventually split into pairs as the pyridyl rotation becomes slow. The ^{19}F spectra of the mononuclear complex $[Pt(C_6F_4CF_3)_2L^1]$ display this effect in the temperature range 303 to 223 K. Bandshape anal-

Table 7 Activation energy data for 1,4-metal-nitrogen shifts in Re^{I}, Pt^{IV} and Pt^{II} complexes of ligands L^1, L^2, L^3 and related ligands

Complex	Populations (%)	$\Delta H^{\ddagger}$/kJ mol^{-1}	$\Delta S^{\ddagger}$/J K^{-1} mol^{-1}	$\Delta G^{\ddagger}$[a]/kJ mol^{-1}	Ref.
$[\{ReBr(CO)_3\}_2L^1]$	50:50	69.7 ± 3.5	−8.7 ± 10.2	72.3 ± 0.5	Present work
$[(PtClMe_3)_2L^1]$	50:50	58.7 ± 1.2	−16.7 ± 3.7	63.7 ± 0.1	″
$[ReBr(CO)_3L^1]$	50:50	64.5 ± 3.6	−22.1 ± 10.1	71.2 ± 0.6	″
$[ReBr(CO)_3PtIMe_3L^1]$	50:50	—	—	70.4(Re)(353 K)[b]	″
				65.3(Pt)(323 K)[c]	″
$[\{Pt(C_6F_4CF_3)_2\}_2L^1]$	50:50	—	—	97.2 ± 0.1(393 K)[d]	″
$[Pt(C_6F_4CF_3)_2L^1]$	50:50	—	—	99.4 ± 0.1(393 K)[d]	″
$[\{ReBr(CO)_3\}_2L^2]$	50:50	69.4 ± 1.9	−13.1 ± 5.2	73.3 ± 0.3	″
$[(PtIMe_3)_2L^2]$	50:50	46.1 ± 0.9	−57.3 ± 3.0	63.1 ± 0.1	″
$[\{Pt(C_6F_4CF_3)_2\}_2L^2]$	50:50	—	—	100.1 ± 0.1(393 K)[d]	″
$[Pt(C_6F_4CF_3)_2L^2]$	50:50	—	—	100.3 ± 0.1(393 K)[d]	″
$[(PtIMe_3)_2L^3]$	32:25:25:18	—	—	65.6(313 K)[e]	″
$[Pt(C_6F_5)_2L^3]$	58:42	—	—	100.0(393 K)[d]	″
$[ReBr(CO)_3(terpy)]$	50:50	79.8 ± 1.7	27.5 ± 4.8	71.6 ± 0.1	16
$[PtClMe_3(terpy)]$	50:50	57.9 ± 1.4	−13.7 ± 4.3	62.0 ± 0.1	17
$[Pt(C_6F_5)_2(terpy)]$	50:50	93.0 ± 2.9	−3.2 ± 7.3	93.9 ± 0.7	15
$[ReBr(CO)_3(mcpt)]$	66:34	74.1 ± 2.9	−0.3 ± 0.1	74.1 ± 0.9	2
$[ReBr(CO)_3(mcpmt)]$	50:50	72.5 ± 2.7	−0.4 ± 8.0	72.6 ± 0.4	2
$[PtIMe_3(mcpt)]$	63:37	72.8 ± 0.6	22.9 ± 1.9	66.0 ± 0.01	2
$[Pt(C_6F_5)_2(mcpt)]$	64.5:35.5	—	—	100.6(393 K)[d]	2

[a] At 298.15 K unless otherwise stated. [b] From coalescence of the exchanging pair A ⇌ J. [c] From coalescence of the exchanging pair L ⇌ S. [d] From 2D-EXSY spectra. [e] From coalescence of the exchanging pair H ⇌ M.

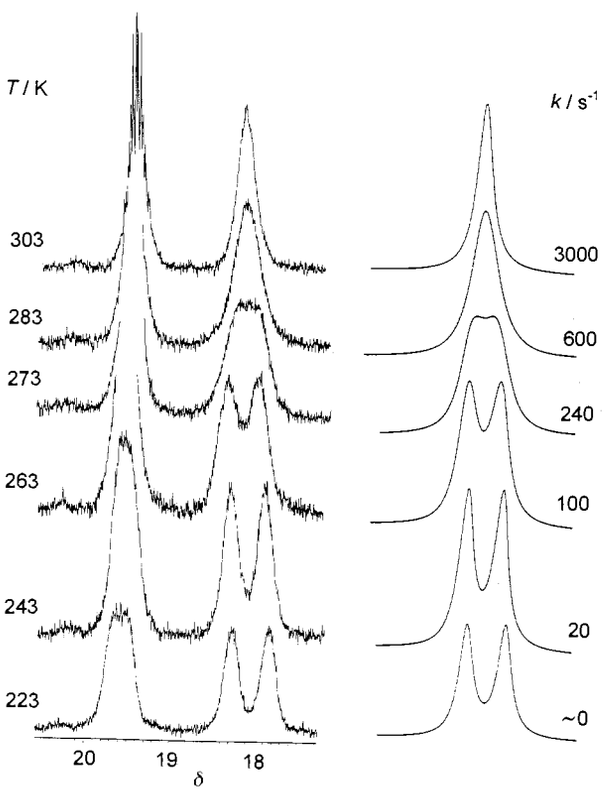

Fig. 9 376 MHz ^{19}F NMR spectra (*meta* ring fluorines only) of $[Pt(C_6F_4CF_3)_2L^1]$ in CD_2Cl_2 in the temperature range 223–303 K. Computer simulated spectra of the signals of the ring adjacent to the pendant pyridyl ring are shown alongside with the 'best-fit' rate constants.

ysis was then carried out on the *meta*-fluorine signal shapes (see Fig. 9). The equal intensities of the pairs of rotamer signals at low temperatures suggest that both rotamers are equivalent and this suggests that the two perfluoroaromatic rings and the pyridyl ring are approximately parallel to each other and all rings are orthogonal to the plane containing the chelated pyridyl rings (Fig. 10).

The 4-position ring or CF_3 fluorines lie on average in this plane and so are quite insensitive to the pendant pyridyl rotation in the mononuclear complexes $[Pt(C_6F_4CF_3)_2L^1]$ and $[Pt(C_6F_4CF_3)_2L^2]$. However, a comparable low temperature

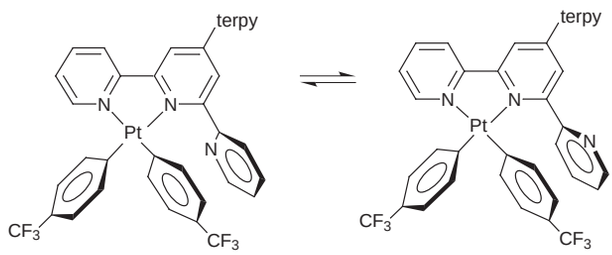

Fig. 10 Proposed solution rotamers of $[Pt(C_6F_4CF_3)_2L^1]$.

study of the dinuclear complex $[\{Pt(C_6F_4CF_3)_2\}_2L^1]$ revealed, in addition to the expected changes in the ring fluorine signals, a broadening and eventual splitting (of *ca.* 5 Hz) of the CF_3 triplet signal. This is attributed to the fact that the two pendant pyridyl rings can become locked at low solution temperatures with their N-heteroatoms either *syn* or *anti* with respect to each other. In principle all the ring fluorine or CF_3 signals should reflect this conformational isomerism. In practice, however, it is likely to affect only those fluorines on the rings adjacent to the pendant pyridyl. In the present case this is seen in the CF_3 signals only.

Such sensitivity to the long range spatial relationship of the locked pyridyl rings is lost when a phenyl spacer group is inserted between the two terpy fragments in the L^2 ligand complexes. Thus, the low temperature ^{19}F spectra of $[\{Pt(C_6F_4CF_3)_2\}_2L^2]$ show the expected splitting effects of the ring-fluorine signals on cooling but no effect on the CF_3 signal suggesting no magnetic communication between the two sides of the dinuclear complex.

Discussion

The activation energy data for the 1,4-metallotropic shift in these Re^{I}, Pt^{IV} and Pt^{II} complexes of 'back-to-back' terpy ligands are collected in Table 7 and corresponding values for terpy, mcpt and mcpmt complexes included for comparison purposes [mcpmt = 4′-(4-chlorophenyl)-4,4″-dimethyl-2,2′:6′,2″-terpyridine]. It will be seen that the activation energies (expressed as $\Delta G^{\ddagger}$ values) for all these terpyridyl-based ligand complexes fall within very narrow ranges for each transition metal, these ranges being 62–66 kJ mol^{-1} for Pt^{IV} complexes, 70–74 kJ mol^{-1} for Re^{I} complexes and 94–101 kJ mol^{-1} for Pt^{II} complexes. Such an energy ordering has been noted before in other series of complexes[2,15] and is clearly a function primarily of the transition metal rather than the ligand.

Table 8 Activation parameters for restricted rotation of the pendant pyridyl rings in mono- and di-nuclear Pt^{II} complexes of L^1, L^2 and others

Complex	T range[a]/K	$\Delta H^{\ddagger}$/kJ mol^{-1}	$\Delta S^{\ddagger}$/J K^{-1} mol^{-1}	$\Delta G^{\ddagger}$[b]/kJ mol^{-1}	Ref.
$[Pt(C_6F_4CF_3)_2L^1]$	203–293[c]	45.3 ± 1.8	−32.6 ± 6.5	55.0 ± 0.2	Present work
$[\{Pt(C_6F_4CF_3)_2\}_2L^1]$	273[d]	—	—	54.4 ± 0.1[d]	″
$[Pt(C_6F_4CF_3)_2L^2]$	213–283[c]	27.8 ± 0.8	−89.8 ± 3.3	54.5 ± 0.2	″
$[\{Pt(C_6F_4CF_3)_2\}_2L^2]$	213–273[c]	29.1 ± 1.0	−86.5 ± 4.1	54.9 ± 0.2	″
$[Pt(C_6F_5)_2(terpy)]$	253–303	—	—	55.9 ± 0.2	15
$[Pt(C_6F_4CF_3)_2(TPT)]$	193–243	45.1 ± 2.0	9.2 ± 9.3	42.3 ± 0.7	3

[a] Solvent CD_2Cl_2. [b] At 298.15 K. [c] Values based on bandshape analysis of exchanging *meta* ring F signals. [d] Value based on the coalescence temperature given.

There is no systematic difference in activation energies for corresponding L^1, L^2 and L^3 ligand complexes. However, it should be noted that values for these 'back-to-back' terpy ligand complexes are generally slightly higher (by up to 6 kJ mol^{-1}) than the corresponding terpy ligand complexes. This, therefore, does imply some slight electronic influence between the two sides of the complex perhaps influencing the M–N bond of the central pyridyl ring. However, this point should not be made too strongly as this activation energy difference does not apply when comparison is made with the substituted terpy ligand, mcpt or mcpmt. Furthermore, there is no significant difference in energies between the fluxions in the mononuclear and dinuclear complexes, implying that the metallotropic shifts are primarily independent of the nature of the opposite side of the ligand, *i.e.* whether it be metal coordinated or not.

The results of the restricted rotation studies of the pendant pyridyl rings are quite predictable. Values for Pt^{II} complexes of L^1 and L^2 ligands are given in Table 8 and compared with corresponding terpy[15] and TPT[3] complexes. $\Delta G^{\ddagger}$ values fall within the narrow range 54–56 kJ mol^{-1} with the exception of TPT which is significantly lower. There was evidence in the ambient temperature spectra of $[\{ReBr(CO)_3\}_2L^1]$ of considerable restriction to rotation of the pyridyl rings. However, this was not easily quantified but our observations suggest that the energy barrier would be significantly higher than in the corresponding terpy complexes.[16]

The main conclusions of this work are that the well established 1,4-metallotropic shifts in bidentate chelate terpyridine-based complexes are sensitive only to the local metal-coordination environment, and there is negligible steric or electronic interaction between the two sides of 'back-to-back' terpyridine ligands with or without phenyl spacer groups. Likewise, rotations of the pendant pyridyl rings are not influenced by the presence of the other terpy fragment whether it be metal coordinated or not.

Acknowledgements

We wish to thank the EPSRC for a postgraduate research fellowship (to A. G.), for a research studentship (to M. D. O.) and for use of the national mass spectrometry service at the University of Wales, Swansea.

References

1 E. C. Constable, *Adv. Inorg. Chem. Radiochem.*, 1986, **30**, 69.
2 A. Gelling, K. G. Orrell, A. G. Osborne and V. Šik, *J. Chem. Soc., Dalton Trans.*, 1998, 937 and refs. therein.
3 A. Gelling, M. D. Olsen, K. G. Orrell, A. G. Osborne and V. Šik, *Inorg. Chim. Acta*, 1997, **264**, 257.
4 H. D. Kaesz, R. Bau, D. Hendrickson and J. M. Smith, *J. Am. Chem. Soc.*, 1967, **89**, 2844.
5 D. H. Goldsworthy, Ph.D. Thesis, University of Exeter, 1980.
6 G. Lopez, G. Garcia, N. Cutillas and J. Ruiz, *J. Organomet. Chem.*, 1983, **241**, 269.
7 F. A. Cotton, *J. Am. Chem. Soc.*, 1961, **83**, 344.
8 B. R. Steele and K. Vrieze, *Transition Met. Chem.*, 1977, **2**, 140.
9 K. T. Potts, D. A. Usifer, A. Guadalupe and H. D. Abruna, *J. Am. Chem. Soc.*, 1987, **109**, 3961; K. T. Potts, P. Ralli, G. Theodoridis and P. Winslow, *Org. Synth.*, 1986, **64**, 189.
10 E. C. Constable and A. M. W. Cargill-Thompson, *J. Chem. Soc., Dalton Trans.*, 1992, 3467.
11 D. F. Shriver, *Manipulation of Air-Sensitive Compounds*, McGraw Hill, New York, 1969.
12 D. A. Kleier and G. Binsch, DNMR3 Program 165, Quantum Chemistry Program Exchange, Indiana University, IN, 1970.
13 E. W. Abel, T. P. J. Coston, K. G. Orrell, V. Šik and D. Stephenson, *J. Magn. Reson.*, 1986, **70**, 34.
14 V. Šik, Ph.D. Thesis, University of Exeter, 1979.
15 E. W. Abel, K. G. Orrell, A. G. Osborne, H. M. Pain, V. Šik, M. B. Hursthouse and K. M. A. Malik, *J. Chem. Soc., Dalton Trans.*, 1994, 3441.
16 E. W. Abel, V. S. Dimitrov, N. J. Long, K. G. Orrell, A. G. Osborne, H. M. Pain, V. Šik, M. B. Hursthouse and M. A. Mazid, *J. Chem. Soc., Dalton Trans.*, 1993, 597.
17 E. W. Abel, V. S. Dimitrov, N. J. Long, K. G. Orrell, A. G. Osborne, V. Šik, M. B. Hursthouse and M. A. Mazid, *J. Chem. Soc., Dalton Trans.*, 1993, 291.

Paper 8/05300F